Femtosecond time resolved CARS spectroscopy of H2-N2 mixtures in the Dicke regime: Experiments and modeling of velocity effects

Ha Tran, Frédéric Chaussard, N. Le Cong, B. Lavorel, O. Faucher, Pierre Joubert

Femtosecond time resolved CARS spectroscopy of H_2-N_2 mixtures in the Dicke regime: Experiments and modeling of velocity effects

H. Tran[1#], F. Chaussard[2], N. Le Cong[2], B. Lavorel[2], O. Faucher[2], and P. Joubert[3]

[1]Laboratoire Inter-universitaire des Systèmes Atmosphériques (LISA)
UMR CNRS 7583, Universités Paris VII et Paris XII, 94010 Créteil Cedex France
[2]Institut Carnot de Bourgogne, UMR CNRS 5209, Université de Bourgogne, 9 Avenue Alain Savary, BP 47870, F-21078 Dijon Cedex, France
[3]Institut UTINAM, UMR CNRS 6213, Université de Franche-Comté, 25030 Besançon Cedex, France.

Abstract

In this paper, we present measurements and modeling of femtosecond time resolved CARS signal in H_2-N_2 mixtures at low densities. Three approaches have been used to model the CARS response. The first is the usual sum of Voigt profiles. In the second approach, the speed dependent Voigt profile is used. In the last approach, a new model of the CARS signal is developed which takes into account the velocity changes induced by collisions and the speed dependence of the collisional parameters. The velocity changes are modeled using the Keilson and Storer memory function; the radiator speed dependences of the collisional parameters are determined from their temperature dependences. The results show that the changes of the velocity have important effects for the H_2/N_2 system at the Dicke density regime.

Corresponding author: Tel: 33(0)145176558, Fax: 33(0)145171564 Email: hatran@lisa.univ-paris12.fr

1. Introduction

Nonlinear Raman spectroscopy techniques, especially CARS, have demonstrated for years their powerful performance in terms of temperature and concentration diagnostics. Extensively used in the frequency domain, they are now well-developed in the time domain.[1] The use of ultra short lasers pulses offers complementary information with regard to molecular structures and chemical reaction dynamics, and has several advantages, such as the suppression of the off-resonant contribution to the CARS signal when the pump and the probe are delayed, and the possibility of performing measurements with high repetition rates.

Hydrogen is a molecule of particular interest in combustion diagnostic, especially in thermometry in H_2/air flames. Both exhaustive experimental and theoretical studies[2-7] have shown the importance of inhomogeneous effects on spectral lineshapes from the Doppler to the collisional regime in H_2-X (X=Ar, N_2, H_2O …) binary mixtures and their consequences on the diagnostic accuracy. The origin of these effects, that also exist in other molecules[8-12] but are enhanced in H_2 due to its lightness, has to be found in the radiator speed dependence of the collisional parameters, coupled to the velocity changes due to collisions. Several line-shape models have been developed in the frequency domain to account for these effects.[13] Among them, a kinetic model is particularly interesting since it accounts for the speed dependence of the collisional line parameters and allows a relatively simple description of the velocity changes. This kinetic model is based on the time evolution of the autocorrelation function in which the Keilson-Storer function represents the velocity changes due to collisions. It was successfully tested for different systems under various conditions of temperature and pressure.[11,14,15] A first modeling of the time-resolved CARS response taking into account these velocity effects has been proposed previously by the present authors[16] for the H_2/N_2 system, but it was limited to the collisional regime (high pressures). For such a situation, the Doppler effect can be neglected and, hence, the velocity orientation

changes can be disregarded, so that only the changes of the velocity modulus need to be accounted for. The resulting mono-dimensional model developed, called KS-1D model, leads to satisfactory results both for comparisons between measured and calculated signatures and for temperature diagnostics. The present work extends this approach to the low density regime where changes of both velocity orientation and modulus have to be considered.

This paper is organized as follows: In Sec. II, the time resolved experimental set-up and the experimental conditions are recalled. Sec. III is devoted to the description of the KS-3D bi-parametric model, and Sec. IV presents the analysis of the experimental data. Discussion and concluding remarks are given in Sec. V.

2. Experimental set-up

In the CARS experiment, the Q-branch $(v = 0, J) \rightarrow (v = 1, J)$ transitions of H_2 are excited by two femtosecond laser pulses, the pump and the Stokes, respectively centered at 600 nm and 800 nm. A third pulse, the probe, tuned to 600 nm and arriving after a time delay t, allows for the generation of an Anti-Stokes signal, centered at 480 nm, thanks to the interaction with the third-order nonlinear susceptibility of the gas medium. The laser system delivering the ultrashort pulses is a 1 kHz (chirped pulsed amplified) Ti:sapphire femtosecond laser operating at 800 nm. Its output beam is split in two parts: one part is used as the Stokes beam (100 fs pulse duration, 10 nm bandwidth) and the second part is used, after frequency doubling, as a pump beam for a noncolinear optical parametric amplifier (NOPA). The NOPA, after splitting of its output beam, delivers the pump and probe pulses (40 fs pulse duration, 25 nm bandwidth). The pump and Stokes beams are synchronized by a first delay line, and the time delay between these last two excitation pulses and the probe beam is controlled by a second delay line that can perform scans up to 600 ps. All three pulses are linearly polarized and parallel, and are focused in the gas cell by means of a 450

mm focal lens. The so-called folded BOXCARS configuration is used so as to fulfil the phase matching condition and to allow for a good spatial separation of the CARS signal beam. The latter is selected by a diaphragm, collimated by a 400 mm focal lens and sent onto a photomultiplier for detection. The signal is generally averaged over 50 laser shots for each pump-probe delay. The measurements were performed at three temperatures, 296, 503 and 703 K, at densities close to those of the Dicke regime, ie. from 0.5 to 2.0 amagats, where both Doppler and collisional effects have to be considered. The densities are calculated from the measurement of the pressure and temperature of the studied gas sample and by using a state equation based on the second Virial correction for non ideal gases. Various H_2-N_2 mixtures were studied, with H_2 mole fractions of 10, 20 and 50%.

3. Theoretical calculation: The KS-3D bi-parametric model

In this section, we present the model used to calculate the CARS signal. As shown in Refs. [15 and references therein], in the frequency domain, in a system such as H_2/N_2 for which the perturber is much heavier than the radiator, the changes of the radiator velocity have significant effects on the spectral line-shape. Furthermore, the collisional shifting value is particularly important, more than two times the broadening, and strongly depends on the relative speed. These features lead to various changes of the spectral line shapes with respect to the usual Voigt profile. In particular, the spectrum becomes strongly asymmetric and the line broadening and shifting coefficients are non linear functions of the perturber mole fraction. In order to model these effects, a kinetic model based on the time evolution of the autocorrelation function using the Keilson-Storer description of velocity changes[17] was developed. In the time domain, the first results were obtained in the collisional regime (high density) for the H_2/N_2 system[16] where only speed (velocity modulus) changes were considered. The results showed that using a sum of Lorentzian profiles does not correctly

model the time response and leads to important errors for temperature diagnostics whereas the Keilson-Storer one dimension (KS-1D) model was in satisfactory agreement with measurements. In the following, we present the corresponding approach extended in order to model the CARS time response at low density, in a regime where both velocity modulus and orientation changes have to be taken into account.

The time response CARS at the pump-probe delay t is described by

$$I(t) \approx \left| \sum_J f_J \exp[(i\Delta E_J/\hbar)\tau] d_J(t) \right|^2 , \qquad (1)$$

where the sum is over all rotational level J. The oscillation amplitudes f_J are proportional to the rotational populations and to the convolution of the pump I_L and the Stokes I_S pulses in the frequency domain

$$f_J = S_J(2J+1) \frac{\exp\left\{-\frac{B_e}{kT} J(J+1)\right\}}{Q} \int I_L(\nu) I_S(\nu - \frac{\Delta E_J}{\hbar}) d\nu . \qquad (2)$$

In Eq. (2), B_e is the rotational constant (B_e = 60.80 cm^{-1} for H_2), S_J is the nuclear spin factor (for H_2, S_J = 1 for even J and S_J = 3 for odd J), Q is the rotational partition function, and T is the temperature. The energy ΔE_J for each rotational level J is given by

$$\Delta E_J = \omega_e - 2\omega_e x_e - \alpha_e J(J+1) + \beta_e J^2 (J+1)^2 , \qquad (3)$$

where ω_e, $\omega_e x_e$, α_e, and β_e are molecular constants. For H_2, ω_e = 4395.2 cm^{-1}, $\omega_e x_e$ = 117.99 cm^{-1}, α_e = 2.993 cm^{-1}, and β_e = 1.53x10^{-3} cm^{-1}.[18]

In Eq. (1), $d_J(t)$ is the normalized autocorrelation function of the polarizability responsible for the J line. Within a classical picture, $d_J(t)$ is given by the integration over the radiator velocity $\vec{v}$ of the corresponding quantity $d_J(\vec{v},t)$, *ie*, introducing the speed $v = \|\vec{v}\|$ and the Euler angles θ and φ defining the orientation of $\vec{v}$:

$$d_J(t) = \iiint d_J(\vec{v},t)d^3\vec{v} = \int_0^{2\pi}\int_0^{\pi}\sin(\theta)\int_0^{+\infty} v^2 d_J(v,\theta,\varphi,t)dvd\theta d\varphi \ . \quad (4)$$

As shown in Ref. [19 and references therein], the (classical) time evolution of $d_J(\vec{v},t)$ is given, when assuming *no correlation* between the changes of the radiator velocity and those of its internal state and neglecting collisional interferences between lines, by the following equation

$$\frac{\partial}{\partial t}d_J(\vec{v},t) = -[\iiint f(\vec{v}',\vec{v})d^3\vec{v}']d_J(\vec{v},t) + \iiint f(\vec{v},\vec{v}')d_J(\vec{v}',t)d^3\vec{v}' \\ -[i\vec{k}.\vec{v} + \Gamma_J^{coll}(v) + i\Delta_J^{coll}(v)]d_J(\vec{v},t) \quad , \quad (5)$$

with the initial condition given by the Maxwell-Boltzmann equilibrium distribution $f_{MB}(\vec{v})$. In Eq. (5), the first two terms account for the effects of the changes of the radiator velocity on the time evolution of $d(\vec{v},t)$. $f(\vec{v},\vec{v}')d^3\vec{v}d^3\vec{v}'$ is thus the probability, per unit time, of a velocity change from $\vec{v}'$ (within a small $d^3\vec{v}'$ volume) to $\vec{v}$ (within a small $d^3\vec{v}$ volume). The third contribution $(i\vec{k}.\vec{v})$ represents the dephasing due to the Doppler effect, $\vec{k}$ being the radiation wave vector. Finally, $\Gamma_J^{coll}(v) + i\Delta_J^{coll}(v)$ takes into account the damping and dephasing of $d_J(\vec{v},t)$ due to collision-induced internal relaxation, $\Gamma_J^{coll}(v)$ and $\Delta_J^{coll}(v)$ being the speed-dependent collisional width and shift of the optical transition.

Within the Keilson-Storer (KS) model for velocity changes, $f(\vec{v},\vec{v}')$ is given by[17]

$$f_{KS}(\vec{v},\vec{v}') = \nu_{VC} \times (1-\gamma_{\vec{v}}^2)^{-3/2} \times f_{MB}\left(\frac{\vec{v}-\gamma_{\vec{v}}\vec{v}'}{\sqrt{1-\gamma_{\vec{v}}^2}}\right) , \quad (6)$$

where ν_{VC} is the frequency of velocity changing collisions, assumed here *independent* of $\vec{v}$, such that $\nu_{VC} = \iint f_{KS}(\vec{v}',\vec{v})d^3\vec{v}'$. Using this last identity, Eq. (5) takes the following form:

$$\frac{\partial d_J(\vec{v},t)}{\partial t} = -\left[\nu_{VC} + i\vec{k}\vec{v} + \Gamma_J^{coll}(v) + i\Delta_J^{coll}(v)\right]d_J(\vec{v},t) + \iiint f_{KS}(\vec{v},\vec{v}')d_J(\vec{v}',t)d^3\vec{v}' \ . \quad (7)$$

According to Refs. 19,20, the Keilson-Storer function can be written as

$$f_{KS}(\vec{v},\vec{v}') = \nu_{VC}\bar{f}_M(x)\sum_{n,\ell,m}\gamma_{\tilde{v}}^{2n+\ell}\bar{L}_n^{\ell+1/2}(x)\bar{L}_n^{\ell+1/2}(x')\times Y_{\ell,m}(\theta,\varphi)Y_{\ell,m}^*(\theta',\varphi') \qquad (8)$$

with $x=(v/\tilde{v})^2$, $x'=(v'/\tilde{v})^2$, $\bar{f}_M(x)=4e^{-x}/\sqrt{\pi}$. In Eq. (8), $Y_{\ell,m}(\theta,\varphi)$ are spherical harmonics, $\bar{L}_n^{\ell+1/2}(x)$ are the normalized generalized Laguerre polynomials.[19,21]

As shown by molecular dynamic simulations,[22] for a system as H_2/N_2, the orientation and the modulus of the velocity change with very different time scales. Therefore their changes may considered as uncorrelated and cannot be governed by a unique KS parameter $\gamma_{\bar{v}}$. Bonamy et al[15,22] have proposed a convenient bi-parametric memory model, where $f_{KS}(\vec{v},\vec{v}')$ is described by the product of $f_m(x,x')$, a function describing the changes of the modulus, and $f_o(\vec{v}^o,\vec{v}^{o\prime})$, associated with the changes of the orientation, ie:

$$f_{KS}(\vec{v},\vec{v}') = \nu_{VC}f_m(x,x')f_o(\vec{v}^o,\vec{v}^{o\prime}), \qquad (9)$$

with

$$\begin{aligned} f_m(x,x') &= \bar{f}_M(x)\sum_n \gamma_m^{2n}\bar{L}_n^{1/2}(x)\bar{L}_n^{1/2}(x') \\ f_o(\vec{v}^o,\vec{v}^{o\prime}) &= \frac{1}{4\pi}\sum_\ell (2\ell+1)\gamma_o^\ell P_\ell(\vec{v}^o,\vec{v}^{o\prime}) = \sum_{\ell,m}\gamma_o^\ell Y_{\ell,m}(\theta,\varphi)Y_{\ell,m}^*(\theta',\varphi') \ . \end{aligned} \qquad (10)$$

The products of the $Y_{\ell,m}(\theta,\varphi)$ and $\bar{L}_n^{1/2}(x)$ are thus the eigenfunction of $f_{KS}(\vec{v},\vec{v}')$ with the eigenvalues $\gamma_m^{2n}\gamma_o^\ell$. Note that these functions verify the following ortho-normalization relations[19,21]

$$\begin{aligned} &\int_0^\infty \bar{f}_M(x)\bar{L}_n^{1/2}(x)\bar{L}_{n'}^{1/2}(x)\frac{\sqrt{x}}{2}dx = \delta_{n',n} \\ &\int_0^{2\pi}\int_0^\pi \sin(\theta)Y_{\ell,m}(\theta,\varphi)Y_{\ell',m'}^*(\theta,\varphi)d\theta d\varphi = \delta_{m',m}\delta_{\ell',\ell} \ , \end{aligned} \qquad (11)$$

where z* designates the complex conjugate of z. The autocorrelation function can be also expanded over these basis :

$$d_J(v,\theta,\varphi,t) = \bar{f}_M(x)\sum_{n,\ell,m} a^J_{n,\ell,m}(t)Y_{\ell,m}(\theta,\varphi)\bar{L}^{1/2}_n(x)\,. \qquad (12)$$

Introducing Eq. (12) into Eq. (4) and using the ortho-normalization relations [Eq. (11)], one has

$$d_J(t) = \tilde{v}^3\int_0^{2\pi}\int_0^{\pi}\sin(\theta)\int_0^{+\infty}\bar{f}_M(x)\sum_{n,\ell,m} a^J_{n,\ell,m}(t)Y_{\ell,m}(\theta,\varphi)\bar{L}^{1/2}_n(x)\frac{\sqrt{x}}{2}dx d\theta d\varphi = \tilde{v}^3 a^J_{0,0,0}(t)\ . \qquad (13)$$

In order to simplify notations, the J index will be omitted from now on. Similarly to what has been done in Ref. 19, we now introduce Eq. (12) into Eq. (7), multiply both sides of Eq. (7) by $Y^*_{\ell_0,m_0}(\theta,\varphi)\bar{L}^{1/2}_{n_0}(x)$, integrate over all velocities $\vec{v}$ [ie $d^3\vec{v} = \tilde{v}^3\frac{\sqrt{x}}{2}dx\sin(\theta)d\theta d\varphi$)], and then use the ortho-normalization relations given by Eq. (11). After some algebra, this leads to

$$\begin{aligned}\frac{d}{dt}a_{n_0,\ell_0,m_0}(t) = &-\nu_{VC}\left(1-\gamma_o^{\ell_0}\gamma_m^{2n_0}\right)a_{n_0,\ell_0,m_0}(t) - \sum_n a_{n,\ell_0,m_0}(t)\left[\Gamma_{n_0,n}+i\Delta_{n_0,n}\right]\\ &-i\Delta\omega_D\left[C_{\ell_0,m_0}\sum_n a_{n,\ell_0-1,m_0}(t)I_{n_0,n} + C_{\ell_0+1,m_0}\sum_n a_{n,\ell_0+1,m_0}(t)I_{n_0,n}\right],\end{aligned} \qquad (14)$$

with $C_{\ell_0,m_0} = \sqrt{\dfrac{\ell_0^2 - m_0^2}{(2\ell_0+1)(2\ell_0-1)}}$, and

$$\begin{aligned}\Gamma_{n_0,n} + i\Delta_{n_0,n} &= \int_0^{\infty} dx\bar{f}_M(x)\bar{L}^{1/2}_{n_0}(x)\left[\Gamma^{coll}(x)+i\Delta^{coll}(x)\right]\frac{\sqrt{x}}{2}\bar{L}^{1/2}_n(x)\\ I_{n_0,n} &= \int_0^{\infty} dx\frac{x}{2}\bar{f}_M(x)\bar{L}^{1/2}_{n_0}(x)\bar{L}^{1/2}_n(x)\quad .\end{aligned} \qquad (15)$$

Note that practical ways to calculate $\Gamma_{n_0,n}$, $\Delta_{n_0,n}$, and $I_{n_0,n}$ using recurrence relations of Laguerre polynomials can be found in Ref. 19.

Since all terms in Eq. (14) are diagonal in m_0 and since only the $m_0 = 0$ component of $a_{n_0,\ell_0,m_0}(t)$ contributes to the line shape [Eq. (13)], m_0 will be omitted from now on. Equation (14) can then be written under the simple form

$$\frac{d}{dt}a_{n_0,\ell_0}(t) = -\sum_{n,\ell=\ell_0,\ell_0\pm1} K^{\ell_0,\ell}_{n_0,n}a_{n,\ell}(t)\ , \qquad (16)$$

where the non-zero elements of the **K** matrix are given by

$$
\begin{aligned}
K_{n_0,n}^{\ell_0,\ell_0} &= \nu_{VC}(1-\gamma_{\tilde{v}}^{2n_0+\ell_0})\delta_{n_0,n} + \Gamma_{n_0,n} + i\Delta_{n_0,n} \quad , \\
K_{n_0,n}^{\ell_0,\ell_0-1} &= i\Delta\omega_D \frac{\ell_0}{\sqrt{4\ell_0^{\,2}-1}} I_{n_0,n} \quad , \\
K_{n_0,n}^{\ell_0,\ell_0+1} &= i\Delta\omega_D \frac{\ell_0+1}{\sqrt{(2\ell_0+3)(2\ell_0+1)}} I_{n_0,n} \quad .
\end{aligned}
\tag{17}
$$

If **S** is the matrix of the eigenvectors of **K**, the $a_{0,0}(t)$ component can be expressed as

$$
a_{0,0}(t) = \left(\exp[-Kt]\right)_{0,0}^{0,0} = \sum_k \sum_q S_{0,0,k,q} \exp(-D_{k,q}t)(S^{-1})_{k,q,0,0} \, , \tag{18}
$$

where the diagonal **D** matrix is given by $\mathbf{D} = \mathbf{S}^{-1}\mathbf{K}\mathbf{S}$. As in Eq. (1) all J values have to be considered, leading to $a_{0,0}^{J}(t)$. Combining Eqs. (1) and (18), the derivation of the CARS intensity is straightforward.

From Eq. (7), we can easily obtain the usual Voigt profiles by considering ν_{VC}=0 (no velocity changing) and neglecting the speed dependence of the line broadening and shifting (ie. $\Gamma^{coll} = \overline{\Gamma}^{coll}(x)$, $\Delta^{coll} = \overline{\Delta}^{coll}(x)$). Taking this speed dependence into account and setting ν_{VC}=0 leads to the speed dependent Voigt profiles.[13]

4. Results and discussions

The calculation of the CARS signal for the H_2-N_2 mixture depends on the parameters γ_m and γ_o describing the radiator velocity changes. Their values have been deduced from molecular dynamic simulations described in Ref. [22] and are equal to 0.92 for γ_m and to 0.41 for γ_o at room temperature. These values have been used for the whole temperature range considered in the present work (296-703 K), since the influence of temperature on γ_m and γ_o is very small.[22] The values of ν_{VC} and of the collisional line parameters Γ^{coll} and Δ^{coll} (for J from 0 to 7) have been determined previously and can be found in Ref. 16 and references

therein. In order to have a good convergence of the calculation, several tests have been made and the results show that the values n_0=80 and ℓ_0=10 are sufficient.

At this step, all parameters needed for calculations are known. For each measured signal, we have performed three calculations; the first one is a sum of Voigt profiles, the second is obtained using speed dependent Voigt profiles, and the last one results from the use of the KS-3D bi-parametric model. In order to compare calculated and measured signals, a scaling factor on the signal amplitude and a constant (base line) have been applied to calculated values and determined form a linear least squares fitting procedure. A time shift has been also used in order to assure the agreement between calculated and measured signal positions at zero delay. As a first example, in figure 1, we present the CARS response for a 20%H_2+80%N_2 mixture at 296 K and a total density of 1.85 amagat. The corresponding deviations between observations and calculations using the different models are also presented in this figure. As it can be observed, the speed independent and speed dependent Voigt profiles strongly underestimate the experiments whereas the KS-3D bi-parametric model is in good agreement with the measured signal. The CARS signals obtained with the two Voigt profiles decrease too quickly with the time delay, and the difference between these models and the measurements increases with the delay. This can be understood by the fact that these models, since they neglect velocity changes, disregard the Dicke narrowing. In the frequency domain, they lead to overestimated line widths, a result which translates, in the time domain, by an overestimated decay of the amplitude of the signal oscillations. Another remark is that at this density regime, the speed dependences of the collisional line parameters have a very small influence on the temporal CARS signal, in contrast with the results obtained in the collisional regime[16] where they play a predominant role. These conclusions are also obtained for other concentration and density conditions as can be seen in Figs. 2 and 3. We can also note that differences between the Voigt profile and experiment increase with

the N_2 concentration. This confirms the fact that velocity changes are essentially due to H_2-N_2 collisions. Nevertheless, even for 50% of H_2 at low density a sum of Voigt profiles can not correctly model the measurement (Fig. 2). Figures 4 and 5 present results obtained at higher temperatures for $50\%H_2+50\%N_2$ where a good agreement is also observed between the KS-3D model and experiments. Note that signal calculated by the sum of Voigt profiles (or speed dependence Voigt profiles) decay too quickly, so that the disagreement of these models with the data is more evident over longer delay ranges. With delay from 0 to 50 ps (more or less, depending on the considered pressure), differences between signals calculated by Voigt profiles and our KS-3D model are not obvious.

In order to have an overall view of the influence of velocity effects on the CARS signal, the total density has been retrieved from measurements using two nonlinear least squares fitting procedures. In the first, the density is adjusted using signals calculated from sum of Voigt profiles, thus neglecting all velocity effects. In the second, the KS-3D bi-parametric model, taking into account velocity changes and the speed dependence of collisional parameters, is used. In figure 6, the densities adjusted by using the KS-3D bi-parametric model are plotted versus the true (measured) densities. These results concern all concentration and temperature conditions. As can be observed, densities determined using the KS-3D bi-parametric are in good agreement with experimental ones. However, note that for the measurements made at the highest temperature and the lowest H_2 concentration and for which the signal to noise ratio is a bit worse, the discrepancy can reach 25%. When using Voigt profiles, adjusted densities are very different from the experimental ones with errors reaching 200%. Furthermore, most of the adjusted densities in this way are negative. This can be explained by the fact that Voigt profiles, since it neglects Dicke narrowing, lead to a overestimated decay of the amplitude of the signal oscillations, an error which is here erroneously corrected though underestimated densities. These results confirm that Voigt

profiles can not correctly model the temporal CARS signal of the H_2/N_2 systems and using this in diagnostic of densities leads to unrealistic values.

5. Conclusions

For the first time, velocity effects in femtosecond CARS experiments at low densities have been pointed out. This work demonstrates that Voigt profiles can not model femtosecond CARS signal at low density. Furthermore, at low density, the non-Voigt features of the signal are principally due to velocity changes, the influence of the speed dependence of collisional parameters is negligible, contrary to the collisional regime where speed dependent Voigt profiles can rather correctly model the CARS signal. The KS-3D bi-parametric model, based on the parameterization of the velocity changes,[15,17] and taking into account the speed dependence of collisional parameters has been used to calculate the temporal CARS signal. The H_2/N_2 system considered is of practical interests for the optical diagnostics and leads to important velocity effects previously detected in the frequency domain. In order to quantify the influence of these effects, density retrievals from measured signals performed using two approaches respectively disregarding and taking into account the influence of the velocity effects. The results show that the velocity changes have a considerable influence on the signal and density retrieval for such the H_2/N_2 system at low densities. This confirms the previous results obtained for H_2-N_2 mixtures in the frequency domain. The agreement between the experimental results and the ones calculated using the KS-3D bi-parametric model is excellent. The KS-3D bi-parametric approach is then validated for modeling time resolved CARS response and thus constitutes a unified model from the Doppler to the collisional regimes both in the frequency and in the time domains for molecular systems such as H_2/N_2. In the future, the KS-3D model can be tested by using more accurate velocity changes (for example, velocity changes determined from molecular dynamic simulations).

Acknowledgement

Dr. J.-M. Hartmann is gratefully acknowledged for very helpful discussions and careful reading of this paper.

References

1. B. Lavorel, H. Tran, E. Hertz, O. Faucher, P. Joubert, M. Motzkus, T. Buckup, T. Lang, H. Skenderovi, G. Knopp, P. Beaud, and H. M. Frey, C. R. Physique **5**, 215 (2004).
2. R. L. Farrow, L. A. Rahn, G. O. Sitz, and G. J. Rosasco, Phys. Rev. Lett. **63**, 746 (1989).
3. J. Ph. Berger, R. Saint-Loup, H. Berger, J. Bonamy, and D. Robert, Phys. Rev. A **49**, 3396 (1994).
4. J. W. Forsman, J. Bonamy, D. Robert, J. Ph. Berger, R. Saint-Loup, and H. Berger, Phys. Rev. A **52**, 2652 (1995).
5. P. M. Sinclair, J. Ph. Berger, X. Michaut, R. Saint-Loup, R. Chaux, H. Berger, J. Bonamy, and D. Robert, Phys. Rev. A **54**, 402(1996).
6. F. Chaussard, X. Michaut, R. Saint-Loup, H. Berger, P. Joubert, B. Lance, J. Bonamy, and D. Robert, J. Chem. Phys. **112**, 158 (2000).
7. F. Chaussard, R. Saint-Loup, H. Berger, P. Joubert, X. Bruet, J. Bonamy, and D. Robert, J. Chem. Phys. **113**, 4951 (2000).
8. P. Duggan, P. M. Sinclair, A. D. May, and J. R. Drummond, Phys. Rev. A **51**, 218 (1995).
9. F. Rohart, A. Ellendt, F. Kaghat, and H. Mader, J. Mol. Spectrosc. **185**, 222 (1997).
10. A. S. Pine, and R. Ciurylo, J. Mol. Spectrosc. **208**, 180 (2001).
11. H. Tran, D. Bermejo, J. L. Domenech, P. Joubert, R. R. Gamache, and J. M. Hartmann, J. Quant. Spectrosc. Radiat. Transf. **108**, 126 (2007).
12. F. Rohart, G. Wlodarczak, J. M. Colmont, G. Cazzoli, L. Dore, and C. Puzzarini, J. Mol. Spectrosc. **251**, 282 (2008).

13. J. M. Hartmann, C. Boulet, and D. Robert, *Collisional effects on molecular spectra. Laboratory experiments and model, consequences for applications* (Elsevier, Amsterdam, 2008).

14. D. Robert, and L. Bonamy, Eur. Phys. J. D **2**, 245 (1998).

15. L. Bonamy, H. Tran, P. Joubert, and D. Robert, Eur. Phys. J. D **31**, 459 (2004).

16. H. Tran, P. Joubert, L. Bonamy, B. Lavorel, V. Renard, F. Chaussard, O. Faucher, and B. Sinardet, J. Chem. Phys. **122**, 194317 (2005).

17. J. Keilson, and J. E. Storer, Quart. Appl. Math. **10**, 243 (1952).

18. G. Herzberg, *Molecular Spectra and Molecular Structure : I. Spectra of Diatomic Molecules* (D. Van Nostrand Company, New-York, 1953).

19. H. Tran, and J. M. Hartmann, J. Chem. Phys., **130**, 094301 (2009).

20. R. F. Snider, Phys. Rev. A **33**, 178 (1986).

21. M. Abramowitz, and I. A. Stegun, *Handbook of mathematical functions* (Dover publications Inc., New-York, 1970).

22. P. Joubert, P. N. M. Hoang, L. Bonamy, and D. Robert, Phys. Rev. A **66** 042508 (2002).

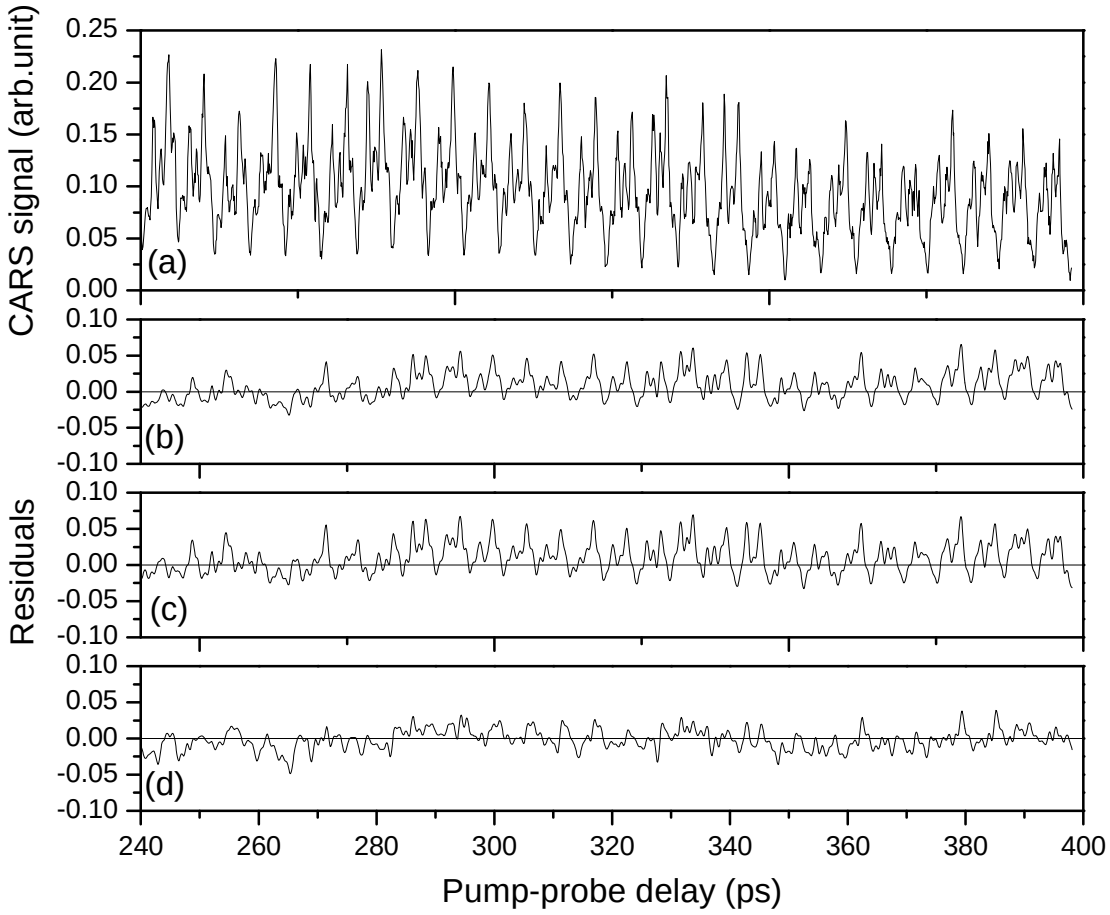

Fig.1 : CARS signal of 20% of H_2 diluted in 80% of N_2 at 296 K and 1.85 amagat. The measurement is shown in the top panel (a). Differences between experiment and signal calculated by a sum of Voigt profiles (b), by a sum of speed dependent Voigt profiles (c) and by the KS-3D bi-parametric model (d) are respectively presented in the lower panels. These differences have been averaged over 0.7 ps in order to reduce the measurement noises.

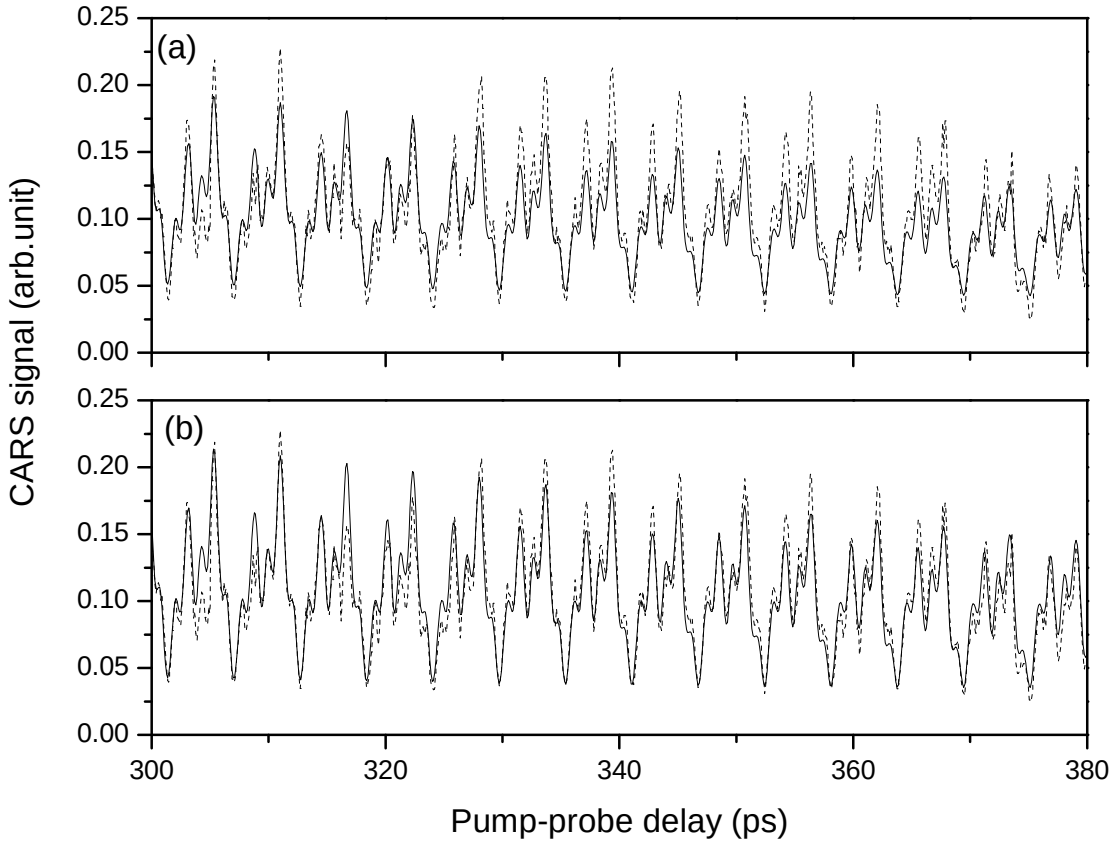

Fig.2 : CARS signal of 50% of H_2 diluted in 50% of N_2 at 296 K and 0.410 amagat. The dash line represents the experimental signal. The full line represents the signal calculated by the Voigt profile (a) and by the KS-3D bi-parametric model (b).

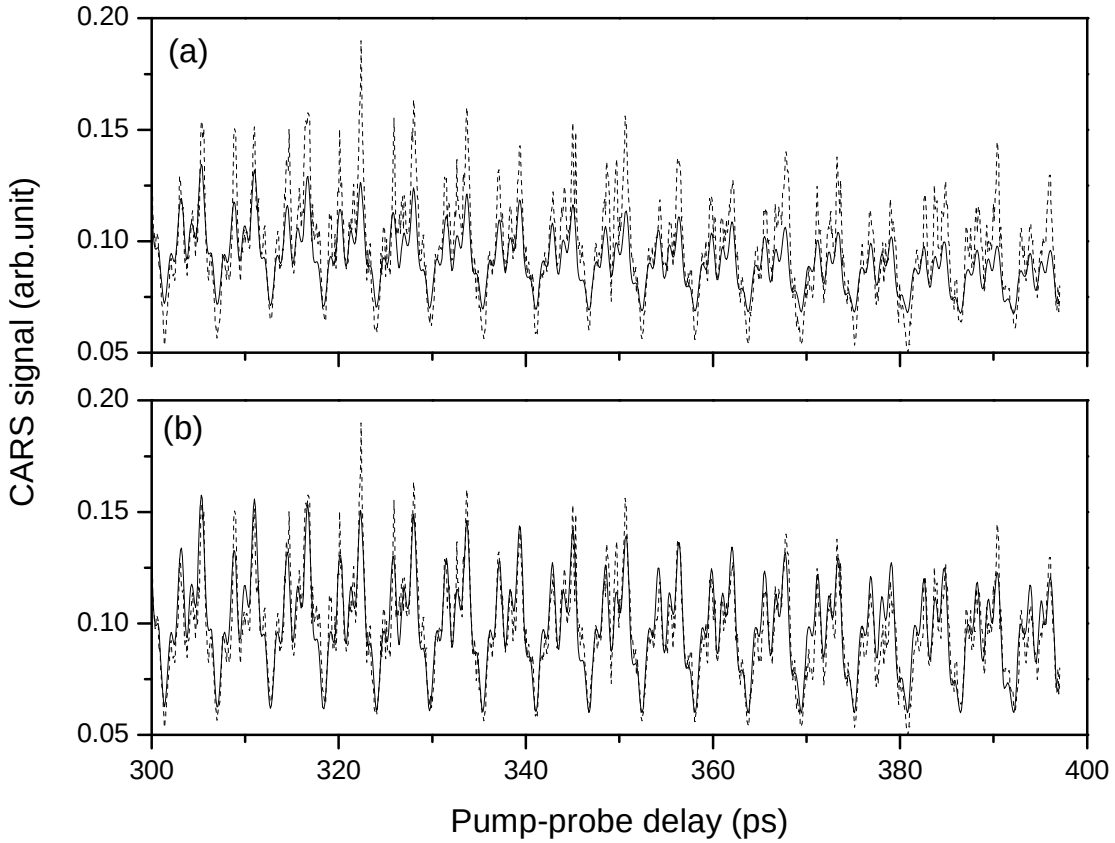

Fig. 3: Same as figure 2 but for a mixture of H_2-N_2 with 20% of H_2 and a density of 0.893 amagat at room temperature.

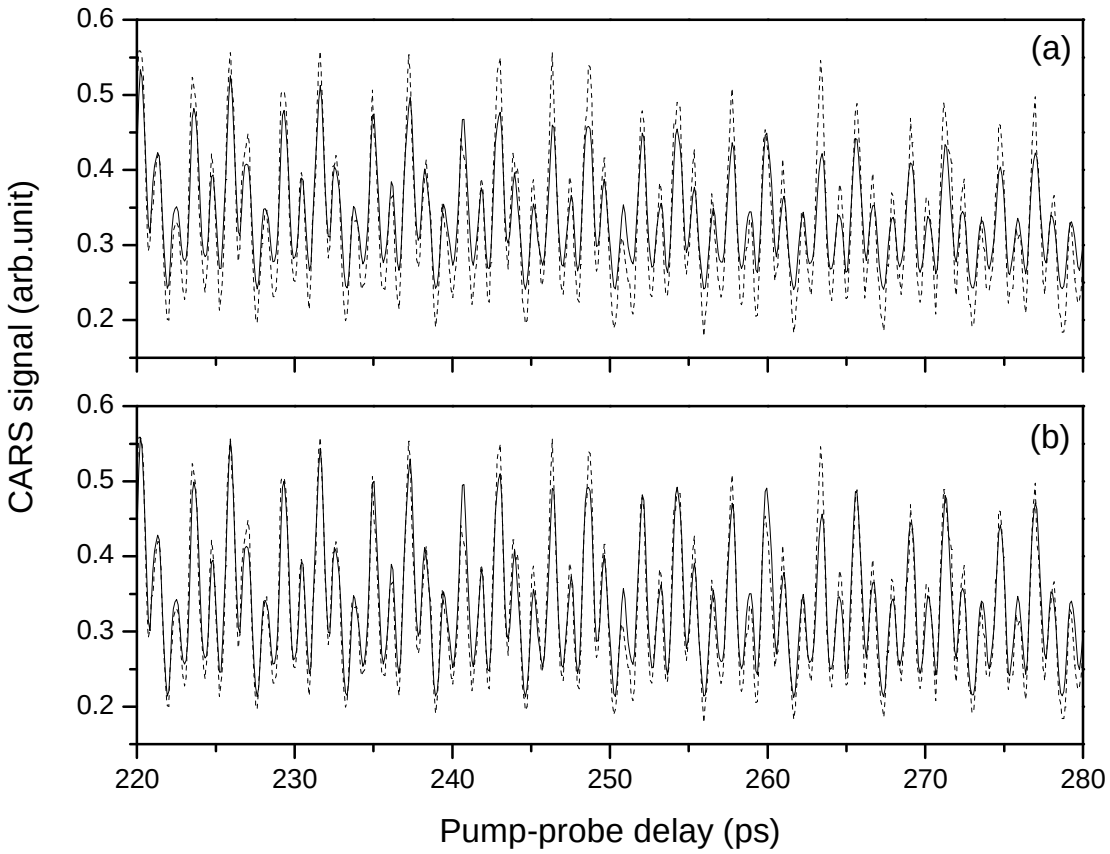

Fig. 4: Same as figure 2 but for a mixture of H_2-N_2 with 50% of H_2 and a density of 0.831 amagat and 503K.

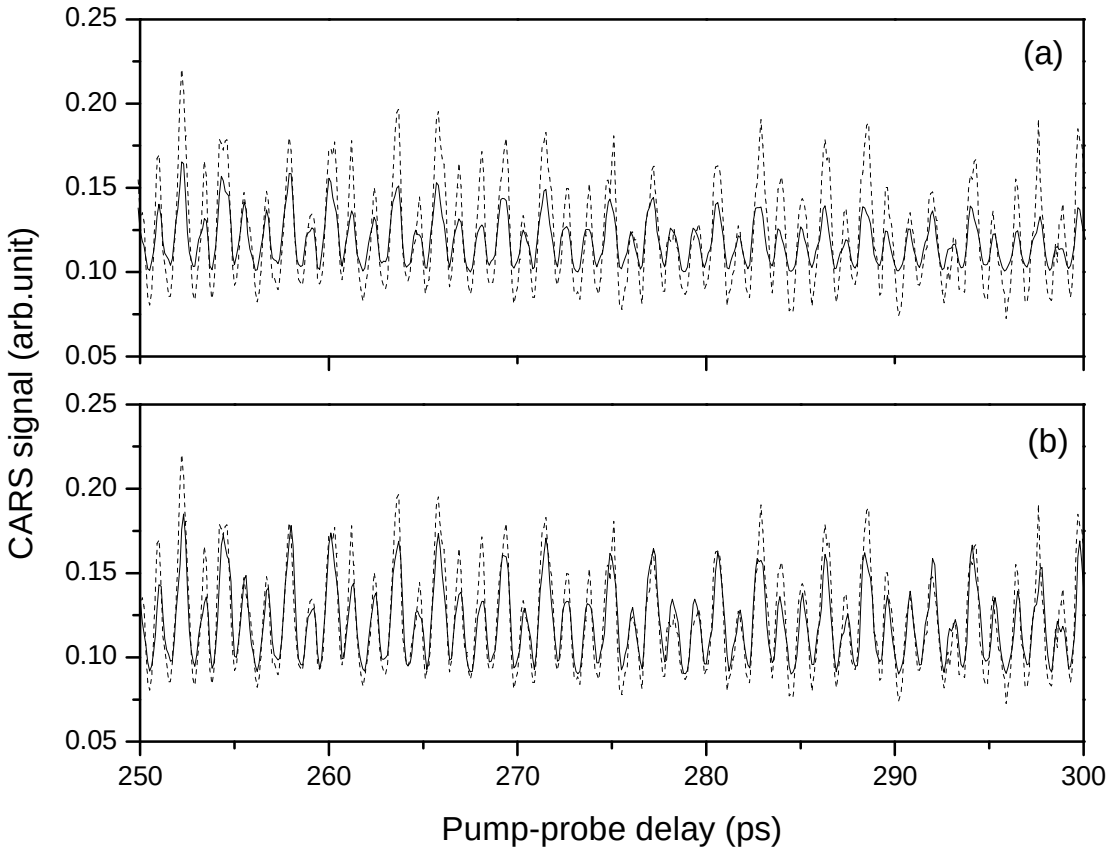

Fig. 5: Same as figure 2 but for a mixture of H_2-N_2 with 50% of H_2 and a density of 0.955 amagat and 703K.

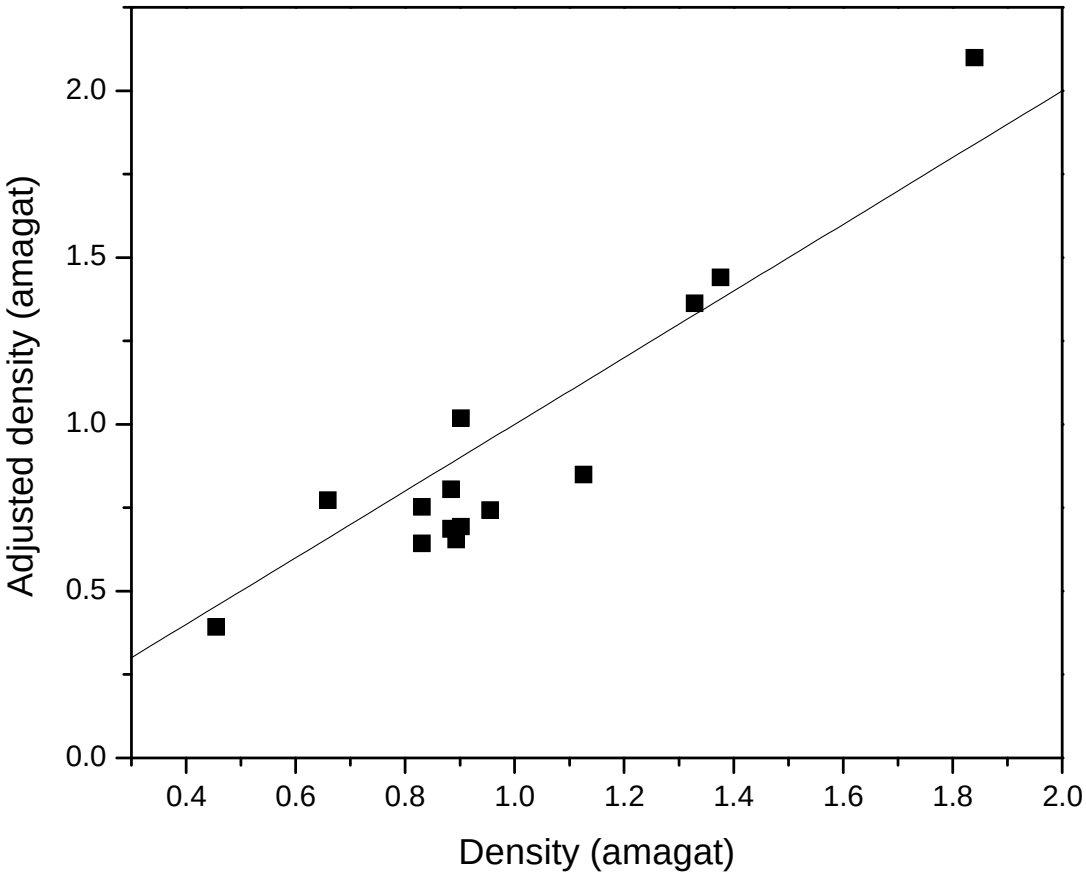

Fig. 6: Densities determined by fitting measured CARS signals in function of the measured density, which is calculated from the gas state equation using the second term Virial correction and from measured pressures. The full squares are results obtained using the KS-3D bi-parametric model. The straight line represents results in which adjusted densities are equal to measured ones